

Mechanism of water-stress induced cavitation in conifers: bordered pit structure and function support the hypothesis of seal capillary-seeding

SYLVAIN DELZON^{1,2}, CYRIL DOUTHE¹, ANNA SALA³ & HERVE COCHARD⁴

¹University of Bordeaux, UMR 1202 BIOGECO, F-33405 Talence, France; ²INRA, UMR 1202 BIOGECO, 69 route d'Arcachon, 33612 Cestas, France; ³Division of Biological Sciences, The University of Montana, Missoula, MT 59812, USA and ⁴INRA, UMR 547 PIAF, F-63100 Clermont-Ferrand, France

ABSTRACT

Resistance to water-stress induced cavitation is an important indicator of drought tolerance in woody species and is known to be intimately linked to the anatomy of the xylem. However, the actual mechanical properties of the pit membrane are not well known and the exact mode of air-seeding by which cavitation occurs is still uncertain. We examined the relationship between cavitation resistance and bordered pit structure and function in 40 coniferous species. Xylem pressure inducing 50% loss of hydraulic conductance (P_{50} , a proxy for cavitation resistance) varied widely among species, from -2.9 to -11.3 MPa. The valve effect of the pit membrane, measured as a function of margo flexibility and torus overlap, explained more variation in cavitation-resistance than simple anatomical traits such as pit membrane, pit aperture or torus size. Highly cavitation resistant species exhibited both a high flexibility of the margo and a large overlap between the torus and the pit aperture, allowing the torus to tightly seal the pit aperture. Our results support the hypothesis of seal capillary-seeding as the most likely mode of air-seeding, and suggest that the adhesion of the torus to the pit border may be the main determinant of cavitation resistance in conifers.

Key-words: bordered pit; cavitation; conifers; drought; torus; xylem.

INTRODUCTION

Conifers are a very important component of terrestrial ecosystems and occur from dry woodlands to the vast boreal forests. Despite their homogenous wood (with only tracheids), conifers exhibit considerable variation in hydraulic

properties; for instance, variation among and within conifer species has been documented in hydraulic conductivity (Domec & Gartner 2002), tracheid size (Pittermann *et al.* 2006a), wood density (Pittermann *et al.* 2006b) and cavitation resistance (Pinol & Sala 2000; Maherali, Pockman & Jackson 2004; Martinez-Vilalta, Sala & Pinol 2004; Brodribb & Cochard 2009).

Because the ascent of water within the secondary xylem of trees involves crossing inter-conduit pit pores, pit structure and function are very important in controlling water movement. Several studies have suggested that resistance to drought-induced embolism is proportional to the ability of pits to prevent air-seeding (Jarbeau, Ewers & Davis 1995; Hacke, Sperry & Pittermann 2004). Indeed, a major cause of xylem cavitation appears to be air leakage from embolized conduits through inter-conduit pits (Crombie, Hipkins & Milburn 1985; Cochard, Cruizat & Tyree 1992; Jarbeau *et al.* 1995). According to this air-seeding hypothesis, cavitation occurs when air bubbles are sucked from a non-functional air filled conduit into a functional conduit through the inter-conduit pits. Because the ability of water to resist air entry through cell wall pores depends on water capillary forces, which, in turn, depend on the diameter of the pore, vulnerability to cavitation increases with increases of the porosity of the pit membranes. Accordingly, variations in xylem anatomical traits among species have been related to cavitation resistance (Hacke *et al.* 2004; Domec, Lachenbruch & Meinzer 2006). In angiosperms, cavitation resistance depends on the size of the largest pores in the pit membranes. Accordingly, greater cell expansion during vessel maturation often results in wider pit area, larger membrane pores and, consequently, lower cavitation resistance (Wheeler *et al.* 2005; Christman, Sperry & Adler 2009).

On the other hand, the inter-tracheid pits of gymnosperms are quite different in structure and function from inter-vessel angiosperm pits, and their roles in cavitation resistance is poorly understood (but see Domec *et al.* 2006; Hacke & Jansen 2009). Gymnosperm inter-tracheid pits are complex and quite specialized (Bailey 1916; Gregory & Petty 1973), and usually consist of circular bordered pits, where the secondary wall arches over the torus-margo pit membrane (Fig. 1; Sachs 1963; Bauch, Liese & Schultze 1972; Hacke

Correspondence: S. Delzon. Fax: +33 (0)5 40 00 36 57; e-mail: sylvain.delzon@u-bordeaux1.fr

Contributors: SD and CD equally contributed to this study and are considered as co-first authors.

Re-use of this article is permitted in accordance with the Terms and Conditions set out at http://wileyonlinelibrary.com/onlineopen#OnlineOpen_Terms

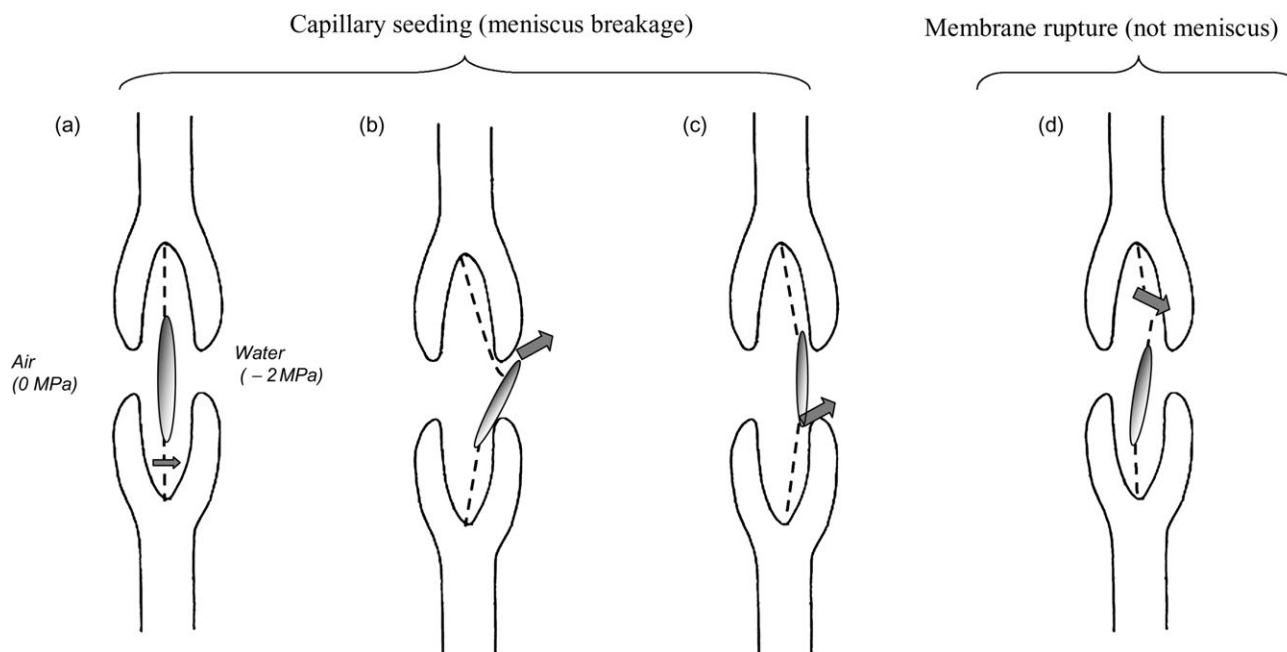


Figure 1. Different hypotheses of air-seeding through a conifer bordered pit membrane: (a) margo capillary-seeding, by capillary rupture of an air/water meniscus through pores in the margo when torus aspiration does not occur; (b) margo stretch-seeding, by elastic stretching allowing the torus to be pulled out through the pit aperture or through membrane slippage that allows the torus to move off-center; (c) seal capillary-seeding, when the torus is not tightly sealed against the pit border (weak aspiration or poor air tightness of torus/pit aperture interface); and (d) margo rupture-seeding, by membrane breakage.

et al. 2004; Pittermann *et al.* 2005). Pit membrane porosity, including that of the torus and margo of conifers, appears to be involved in air-seeding events and is thought to play the most important role in cavitation resistance (Sperry & Tyree 1990; Tyree & Zimmermann 2002). We now know that the essentially impermeable torus has the capacity to exert a valve effect by sealing the pit aperture (Bailey 1916; Pittermann *et al.* 2005). When the pressure difference between the functional and embolized tracheids is high enough, the flexible margo allows the torus to be displaced against the pit border, thereby sealing the pit aperture and preventing subsequent air seeding.

How does cavitation occur with such a pit membrane structure? In a recent overview, Cochard (2006) proposed four different mechanisms of air-seeding in conifers. However, it is currently unknown whether as a general rule, air seeding actually occurs from air bubble being pulled through bordered pit: (1) by capillary rupture of an air/water meniscus through pores in the margo when torus aspiration does not occur (margo capillary-seeding, Fig. 1a); (2) by elastic stretching allowing the torus to be pulled out through the pit aperture or through membrane slippage that allows the torus to move off-centre, exposing a portion of the margo in the pit aperture (margo stretch-seeding, Fig. 1b); (3) when the torus and the inner wall of the pit membrane are not perfectly sealed, allowing air bubbles to pass through pores at the edge of the torus (seal capillary-seeding, Fig. 1c); or (4) by rupture in the membrane when low xylem tensions break the fibrils in the margo (margo rupture-seeding, Fig. 1d). Further, an additional mechanism (Fig. 1c) could also occur

if the torus structure is not fully impermeable allowing an air bubble to pass through tiny pores (Jansen, Pletsers & Sano 2008; Delzon, personal observations).

To our knowledge, only one study has tested the validity of these different modes of air seeding in gymnosperms (Cochard *et al.* 2009), and concluded that, as for angiosperms, water-stress-induced cavitation occurs through capillary-seeding. Indeed, we clearly rejected the margo rupture-seeding hypothesis by membrane breakage (Fig. 1d) and suggested that the capillary failure should occur when the torus is pinned against the pit aperture (Fig. 1c). However, additional research is needed to assess membrane flexibility (margo stretch-seeding) and torus overlap (seal capillary-seeding) and their respective roles in the air-seeding mechanism. Even though previous studies suggested that torus width and pit chamber depth have implications for margo stretch- and rupture-seeding for four conifer species (Domec *et al.* 2006; Hacke & Jansen 2009), the role of pit membrane structure and function in preventing cavitation is poorly understood. A better insight could be gained by examining interspecific variation of pit membrane structure and function and how it relates to xylem hydraulic safety across a wide range of species spanning along large environmental gradients.

In this paper, we examine whether bordered pit structure and function relates to cavitation resistance across conifer species. For the first time we explore the relationship between cavitation resistance and xylem structure and bordered pit anatomy among 40 conifer species varying widely in cavitation resistance. Cavitation resistance was estimated

with the Cavitron technique (Cochard 2002). We studied several bordered pit membrane properties to determine whether the pressure inducing 50% loss of hydraulic conductivity (P_{50}) is directly linked to mechanical and/or functional properties of the pit membrane. The 40 conifer species sampled provided a wide range of cavitation resistance and xylem anatomy, from the dense and highly resistant wood of *Cupressus* to the soft and least resistant wood of *Metasequoia*. We hypothesized that cavitation resistance is strongly dependent on the capacity of the torus to seal the pit aperture as proposed by Petty (1972). We further hypothesized that such sealing effect should depend on: (1) the degree to which the flexibility of the margo allows the displacement of the torus against the overarching border of the pit; and (2) the torus overlap with the pit aperture (i.e. the ratio of the torus to pit aperture diameter). Based on our results, we discuss the likelihood of the different modes of air-seeding proposed in the literature.

MATERIALS AND METHODS

Plant material

During the 2005, 2006 and 2007 spring periods, 40 conifers species representative of a large range of climate dryness were sampled (Appendix S1). Species in six different families were sampled (Farjon 2008): *Araucariaceae* ($n=1$), *Cupressaceae* ($n=12$), *Ginkgoaceae* ($n=1$), *Pinaceae* ($n=23$), *Podocarpaceae* ($n=1$) and *Taxaceae* ($n=2$). Samples were collected in the North America, Europe and Australia from wet to dry habitats in order to have a large range of ecological strategies. Three- to five-year-old branches were sampled in five mature individuals per species in the same stand. Only 40-cm-long straight branches were selected in the upper part of the crown using a telescopic pool-pruner or a slingshot. Immediately after the sampling in the morning, needles were removed and stems were wrapped up with humid paper and conditioned with plastic bags to avoid transpiration. Then, samples were sent to the PIAF laboratory (Clermont-Ferrand, France) and kept refrigerated until measurements.

Vulnerability to cavitation

Within two weeks after receipt of the samples, xylem cavitation was assessed with the CAVITRON, a centrifuge technique following the procedure described by Cochard (Cochard 2002; Cochard *et al.* 2005). Prior to measurement, all branches were cut under water to a standard length of 27 cm, and bark was removed with a razor blade. Branch samples were not flushed prior measurements as we never observed differences in hydraulic conductivity between flushed and unflushed samples in conifers. Samples were infiltrated with a reference ionic solution of 10 mM KCl and 1 mM CaCl₂ in deionized ultrapure water. Centrifugal force was used to generate negative pressure into the xylem and induce cavitation. This method allows to measure xylem conductance under negative pressure. Initially, the

maximum conductance of stem (K_{\max} in $\text{m}^2 \text{MPa}^{-1} \text{s}^{-1}$) was calculated under low xylem pressures (close to zero) (P in MPa). Then, rotation speed of the centrifuge was gradually increased by 0.5 or 1 MPa, to lower xylem pressure. The percentage loss of conductance (PLC) of the stem was determined at each pressure step following the equation:

$$PLC = 100 * \left(1 - \frac{K}{K_{\max}} \right) \quad (1)$$

The relation between P and PLC represents the vulnerability curve of the sample. The curve was adjusted with a sigmoid function (Pammenter & Vander Willigen 1998) using the following equation:

$$PLC = \frac{100}{\left[1 + \exp\left(\frac{S}{25} * (P - P_{50})\right) \right]} \quad (2)$$

where P_{50} (MPa) is the xylem pressure inducing 50% loss of conductance and S (% MPa^{-1}) is the slope of the vulnerability curve at the inflexion point. These two parameters were averaged for each species.

Wood density

To determine whether cavitation resistance varies with wood xylem density (W_d , g cm^{-3}) (Hacke *et al.* 2001), the dry mass per fresh volume of the samples was determined according to Archimedes's principle. A 3-cm-long segment was cut from one end of each sample and submerged in water to measure its fresh volume by water displacement using an analytical balance. Then, samples were dried in an oven at 70 °C until constant weight to determine their dry masses.

Xylem anatomy

One branch out of the five sampled branches per species was randomly selected and used to undertake anatomical measures. Four to five xylem cross sections were cut per sample with a sliding microtome and then fixed on a microscope slide and dyed with safranin. Five photos per section were taken with a digital camera, and analysed with the WinCell® software to measure the lumen area. An average of 500–600 lumens were observed per photo, so an average of 2500–3000 lumens were used to calculate the mean tracheid lumen area for each species (L_a , μm^2).

Pit membranes were observed with a scanning electron microscope (Fig. 2a). Samples were tangentially cut with a sliding microtome and dehydrated during 48 h in an oven (65 °C). Samples were then coated with gold in high vacuum. Pit aperture diameter (D_a , μm), pit membrane diameter (D_m , μm) and torus diameter (D_t , μm) were measured with ImageJ freeware (<http://rsbweb.nih.gov/ij/download.html>; see Fig. 2b for parameter descriptions). On average, 20 observations per parameter and species were done.

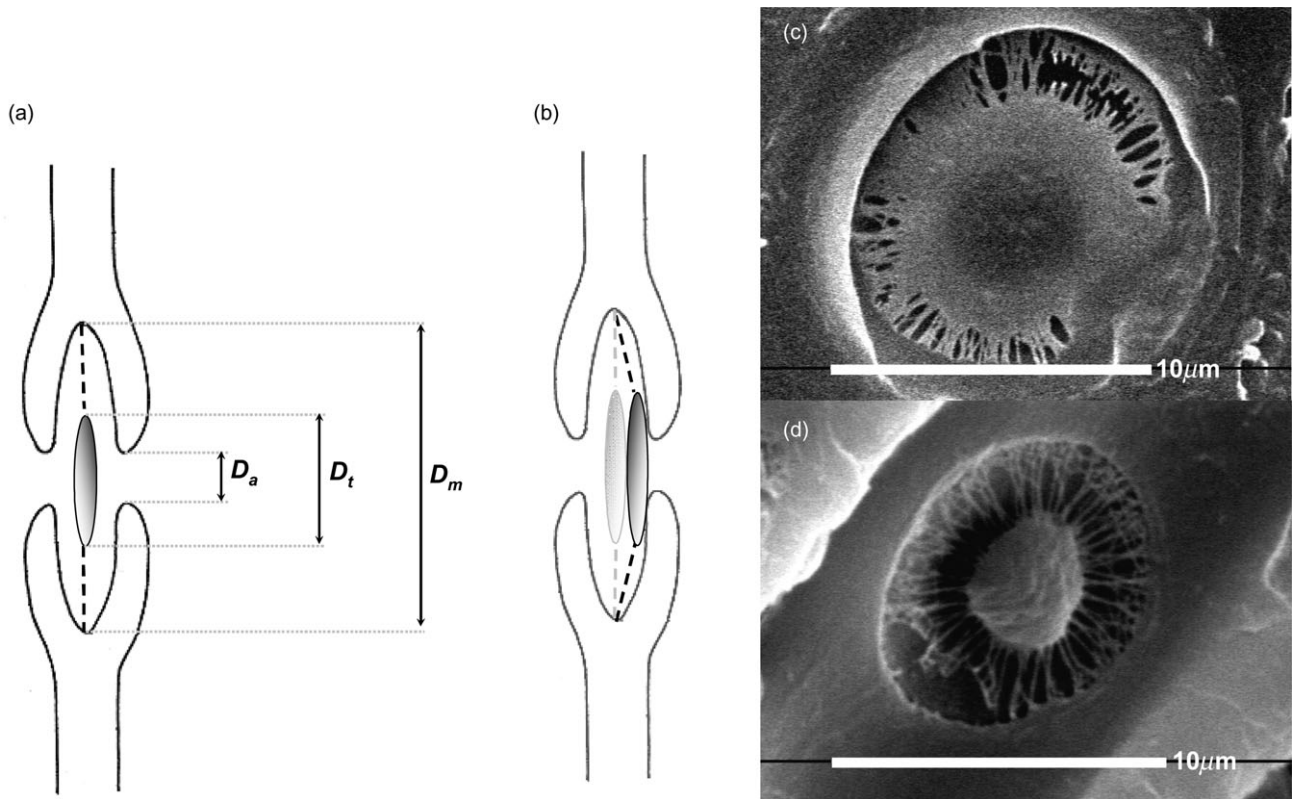


Figure 2. Schematic representation of a bordered pit membrane of conifer on the left. In the first inset (a), important features are represented, namely pit aperture diameter (D_a), torus diameter (D_t) and pit membrane diameter (D_m). The second inset (b) represents the torus valve effect (V_{ef} , i.e. pit aspiration and torus overlap between torus and pit aperture). Torus is both represented in its un-aspirated (grey) and aspirated positions (black). On the right, comparison of bordered pit membrane anatomy between a species vulnerable to cavitation (*P. albicaulis*, c) and a species resistant to cavitation (*C. glabra*, d). White bars represent 10 μm .

Calculation of the valve effect (V_{ef})

In addition to structural properties, we characterized some functional properties of the pit membrane. Firstly, to assess the capacity of movement of the torus inside the pit, the margo flexibility index was estimated by comparing the torus and the pit membrane diameter; this index is inversely proportional to the margo strain at aspiration as defined by Hacke *et al.* (2004). Increasing the torus diameter relatively to pit membrane causes a higher margo flexibility. The margo flexibility index (F) was estimated as follows:

$$F = \frac{(D_m - D_t)}{D_m} \quad (3)$$

Following this equation, when D_t is close to D_m , the length of margo strands is reduced until zero which means that movement of the torus is limited, and so F tends to zero. This index is independent of the pit chamber depth and therefore does not take into account the membrane deflected distance from its flat position.

Secondly, to assess the capacity of the torus to seal the pit aperture during an aspiration event, the torus overlap against the pit aperture (O) was estimated as:

$$O = \frac{(D_t - D_a)}{D_t} \quad (4)$$

When D_t increases in proportion to D_a , the torus is able to seal the pit aperture more efficiently, then O tends to 1.

Following our hypothesis, the capacity of the torus to seal the pit aperture during an aspiration should be both dependent of F and O . The capacity to produce a valve effect (V_{ef}) was calculated as:

$$V_{ef} = F \times O \quad (5)$$

Margo capillary-seeding pressure

To test the hypothesis of margo capillary-seeding (Fig. 1a), we measured the biggest pore in the margo. Measurements of margo porosity were made on the most intact regions of the margo. The diameter of the pore was considered as the diameter of the air bubble. Five pit membranes were studied per species. The capillary seeding pressure of the margo (P_m in MPa, opposite of the pressure sustained by the meniscus) was calculated by the following Young-Laplace equation:

$$P_m = -\frac{4\tau \cos(a)}{D_{mp}} \quad (6)$$

where τ (0.0728 N m⁻¹ at 20 °C) is the water surface tension, a (in degrees) is the contact angle between the microfibrils and the meniscus (assumed equal to zero), and D_{mp} (μ m) is the diameter of the margo pores.

Statistical analysis

Variations of trait values (P_{50} and S) among species and families were assessed using a one-way analysis of variance. Correlations between the different variables were tested with a Pearson correlation coefficient (r). For non linear relations, data were log transformed and negative values

were then converted to positive values. Significant relationships between variables were accepted at $P < 0.05$. Multiple linear regressions were used to determine the combined effect of F and O on P_{50} . Statistical analyses were conducted using the SAS software (version 9.2 SAS Institute, Cary, NC, USA).

RESULTS

Interspecific variation of vulnerability to cavitation

The xylem tension inducing 50% loss in conductivity (P_{50}) dramatically varied among the species ($F = 46.17$, $P < 0.0001$), ranging from -2.91 MPa for *Metasequoia glyptostroboides* to -11.32 MPa for *Cupressus glabra* (Fig. 3;

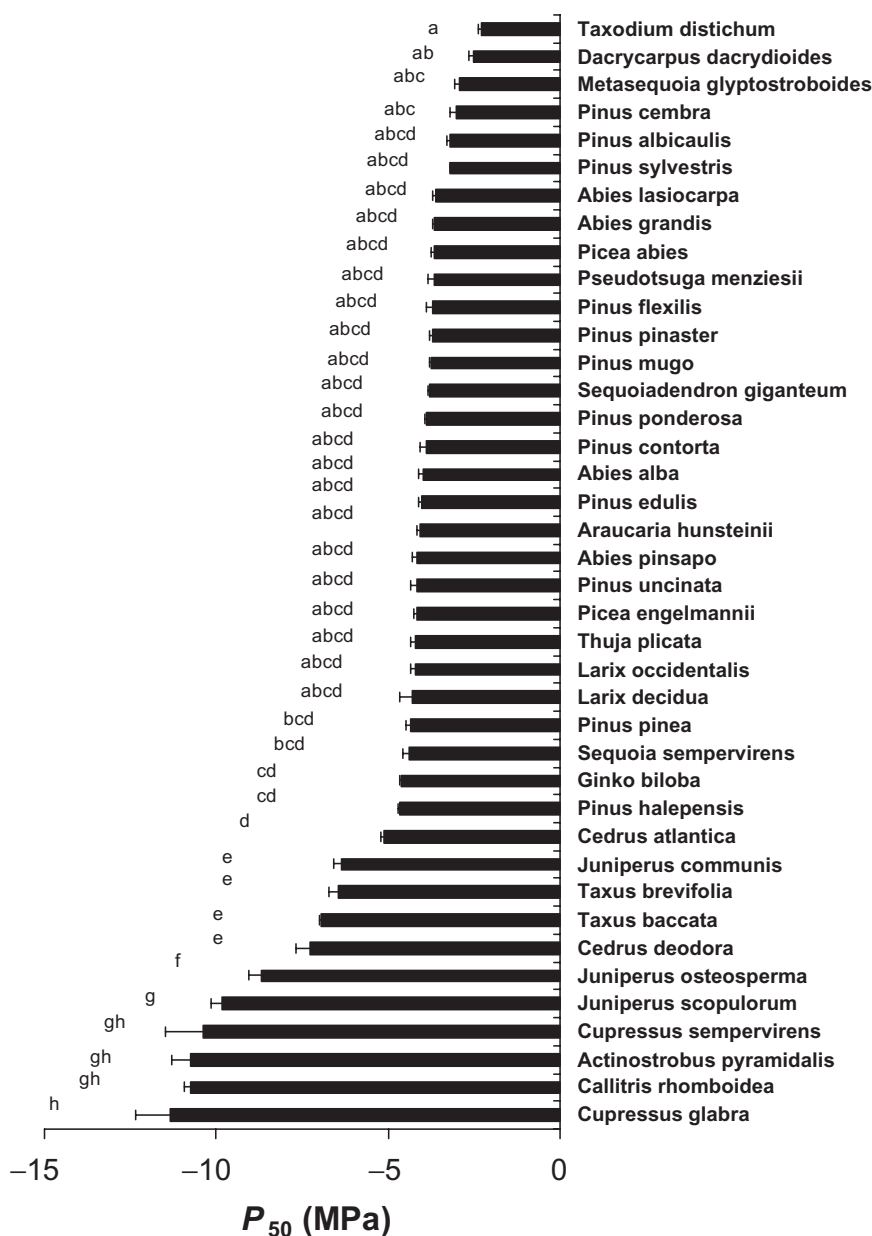


Figure 3. Xylem pressure inducing 50% loss in conductance (P_{50}) measured in 40 conifer species using the Cavitrion technique ($n = 5$ per species). Error bars represent SE. Different letters indicate significant differences between species at $P < 0.05$ (SNK test).

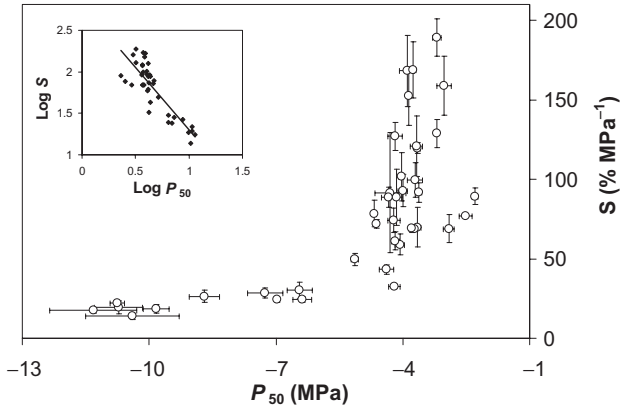


Figure 4. Mean values of vulnerability curve slope (S) versus xylem pressure inducing 50% loss in conductance (P_{50}) measured on 40 species. Error bars represent SE. Log-transformed relationship is shown in the inset.

Appendix S2). The slope of the vulnerability curve (S) also significantly differed among species ($F = 20.01$, $P < 0.0001$), ranging between 13.2% MPa^{-1} (*C. sempervirens*) and 189.2% MPa^{-1} (*Pinus albicaulis*). Values of P_{50} were significantly different between families ($F = 28.10$, $P < 0.0001$) and within families for *Pinaceae* ($F = 29.16$, $P < 0.0001$) and *Cupressaceae* ($F = 24.98$, $P = 0.0001$). We found a strong correlation between P_{50} and S (log transformed data, $r = -0.88$, $P < 0.0001$ (Fig. 4), showing that the rate of embolism decreases as cavitation resistance increases and that species with P_{50} lower than -6 MPa always embolize very slowly (low S).

Wood density and anatomical traits

Wood density (W_d) varied widely between species, from 0.37 to 0.75 g cm^{-3} for *P. pinaster* and *Taxus brevifolia*, respectively (Appendix S2). Not surprisingly, W_d was correlated with all xylem anatomical traits measured (Table 1), highlighting the fact that W_d and tracheids characteristics are mechanically interrelated. The strongest correlations were found with lumen area (L_a) ($r = -0.68$; $P < 0.0001$) and torus diameter (D_t) ($r = -0.60$; $P = 0.0009$), with increases of L_a and D_t as wood density decreases. We also found significant relationships between W_d and pit aperture diameter (D_a) ($r = -0.58$; $P = 0.0011$) and pit membrane diameter (D_m) ($r = -0.45$, $P = 0.02$).

Variables	W_d (g cm^{-3})	L_a (μm^2)	D_m (μm)	D_t (μm)	D_a (μm)
W_d (g cm^{-3})		-0.68***	-0.45*	-0.60***	-0.58**
L_a (μm^2)	-0.68***		0.43*	0.51**	0.37*
D_m (μm)	-0.45*	0.43*		0.90***	0.71***
D_t (μm)	-0.60***	0.51**	0.90***		0.79***
D_a (μm)	-0.58**	0.37*	0.71***	0.79***	

Values indicate Pearson correlation coefficients (r). Bold values indicate significant correlation.

* $P < 0.05$; ** $P < 0.01$; *** $P < 0.001$.

L_a was positively and linearly correlated with D_t ($r = 0.51$; $P = 0.0083$), D_m ($r = 0.43$; $P = 0.02$) and D_a ($r = 0.37$; $P = 0.05$) indicating that tracheids with wide lumens allowing high water transport capacity also have wide pits. Moreover, the structural parameters of pit membranes were strongly and positively correlated between one another (Table 1). Large pit membranes were characterized by large D_t , D_m and D_a .

Concerning the functional properties of the pit membrane, the margo flexibility (F) was correlated with W_d ($r = 0.57$; $P = 0.0018$) and D_a ($r = -0.57$; $P = 0.0015$). Variations of F seemed to be due to D_t variations rather than to D_m . The torus overlap (O) was neither correlated with W_d and L_a , nor with D_m . Its variability was mainly explained by D_a variations. It is worth noticing that L_a was correlated with the pit structural parameters (D_m , D_a and D_t), but not with the pit functional properties (F , O and V_{ef}). Therefore, the functional properties of the bordered pit seemed to be independent of the tracheid size.

Cavitation resistance and xylem structure

P_{50} and S were weakly dependent on xylem structural parameters (Table 2 and Fig. 5) but they were strongly correlated with W_d ($r = -0.60$, $P = 0.0001$ and $r = -0.53$, $P = 0.0009$, respectively). However, this relationship was not significant at the family level or within each family. P_{50} was linearly related with L_a ($r = 0.48$; $P = 0.006$; Fig. 5b), showing that species with a wide tracheid lumen were more vulnerable to cavitation.

Cavitation resistance and bordered pit properties

As shown in Fig. 5, P_{50} and S variations were also positively related with D_a ($r = 0.73$; $P < 0.0001$ for both traits) and D_t ($r = 0.36$; $P = 0.05$ and $r = 0.42$, $P = 0.02$, respectively). However, P_{50} and S were not related to D_m . Using the maximum values of each parameter (e.g. diameter of the largest pit aperture), only some correlations were weakly enhanced (Table 2). To test the margo capillary-seeding hypothesis, we measured the largest pore inside the margo (between microfibrils) and calculated the pressure required to break the meniscus (P_m). Values of P_m were quite high (close to zero) and systematically greater (less negative) than P_{50} values, ranging between -0.4 and

Table 1. Correlations among anatomical traits measured on the 40 conifer species. Wood density (W_d); lumen area (L_a); pit membrane diameter (D_m); torus diameter (D_t); pit aperture diameter (D_a)

Table 2. Correlations between anatomical traits (W_d wood density; L_a lumen area; D_m pit membrane diameter; D_t torus diameter; D_a pit aperture diameter) and cavitation resistance parameters (P_{50} and S)

Anatomical parameters		W_d (g.cm ⁻³)		L_a (μm ²)		D_m (μm)		D_t (μm)		D_a (μm)	
		Mean	Min	Mean	Max	Mean	Max	Mean	Max	Mean	Max
P_{50}	r	-0.60	-0.56	0.48	0.52	0.12	0.05	0.36	0.39	0.73	0.73
	P	0.0001	0.0005	0.006	0.003	0.52	0.78	0.05	0.03	<0.0001	<0.0001
S	r	-0.53	-0.54	0.20	0.16	0.19	0.18	0.42	0.49	0.73	0.76
	P	0.0009	0.0009	0.28	0.40	0.31	0.33	0.02	0.006	<0.0001	<0.0001

Values indicate Pearson correlation coefficient (r) and P value (P). Bold values indicate significant correlations at $P < 0.05$. Underlined values indicate that correlation was more significant using minimum or maximum values instead of mean.

-1.6 MPa (Fig. 6). The functional properties of the bordered pit membrane (F , O and V_{ef}) were strongly correlated with both P_{50} and S (Fig. 7). Increasing margo flexibility or torus overlap increased cavitation resistance. Multiple regression analysis showed that the torus/aperture overlap was the best pit functional property explaining P_{50} variations. Moreover, the steady change in torus/aperture overlap with P_{50} and S is set by the decrease in pit aperture diameter with increasing cavitation resistance, whereas the torus diameter varies modestly (Fig. 5). Finally, relationships between cavitation resistance traits (P_{50} , S) and V_{ef} were stronger than relationships with F and O separately.

DISCUSSION

Inter-specific variability of cavitation resistance in conifers is very large (fourfold), from *C. glabra*, the most resistant species, to *M. glyptostroboides* the least resistant. Such high variability appears to be explained by the functional properties of the bordered pit, specifically the capacity of the torus to seal the pit aperture, which we refer to as valve effect. Species highly resistant to cavitation exhibited a high flexibility of the margo and a large overlap between the torus and the pit aperture, allowing the torus to hermetically seal the pit aperture. In a recent paper, Cochard *et al.* (2009) concluded that margo rupture-seeding was not the determinant of tracheid cavitation and suggested that capillary seeding was the likely mechanism underlying cavitation events in bordered pit membranes. However, the exact location of the capillary failure allowing the entry of air into the tracheid remained enigmatic. As discussed below, our results suggest that such failure occurs at the seal between the torus and the pit aperture.

Margo capillary-seeding

Previous studies have proposed the margo capillary-seeding as a possible mechanism to explain water-stress induced cavitation (Hacke *et al.* 2004; Cochard 2006; Domec *et al.* 2006). According to this hypothesis the margo elasticity is not large enough to allow the torus to move against the pit border (inner wall) to seal the pit aperture. Subsequent increases of xylem tension cause air-water menisci between

margo microfibrils to break allowing air bubbles to embolize adjacent tracheids. The pressure needed to induce this capillary failure depends of the meniscus diameter following the Young-Laplace law. Our results clearly do not support this hypothesis as the capillary seeding pressure of the margo (P_m , calculated with the largest microfibril pore diameter) was systematically and dramatically higher (less negative) than the P_{50} . P_m values ranged between -0.4 and -1.1 MPa and were also higher than the xylem air entry pressure (P_{12} , data not shown), meaning that cavitation never occurred at the pressure inducing capillary failure in the margo. Moreover, Domec *et al.* (2006), for Douglas-fir, estimated the margo deflection pressure (the pressure required to cause the margo to deflect all the way to the pit border) in earlywood and found that the deflection pressure was always higher (less negative) than the capillary seeding pressure of the margo. Therefore, assuming that the margo elasticity is large enough, pit membrane would be deflected and aspirated rather than allowing air seeding through the pores in the margo.

Margo stretch-seeding

Hacke *et al.* (2004) have suggested that the flexibility of the margo could play a role in the mechanism of cavitation, with more vulnerable species having a more flexible margo. High margo flexibility could allow the torus to be pulled out through the pit aperture or to move off-center, exposing a portion of the margo in the pit aperture. Indeed, it was showed for Douglas-fir that the pressure required to stretch the membrane was similar to the cavitation resistance (P_{50}), suggesting that the most likely mode of air seeding is by elastic stretching (Domec *et al.* 2006). Contrary to expectations, our results reported a positive correlation between margo flexibility (F) and cavitation resistance; the higher the margo flexibility, the more cavitation resistant the species (Fig. 7). A high margo flexibility may facilitate the torus to move towards the pit border and improve the seal between the torus and the pit aperture. Moreover, it's worth noticing that the torus area is always larger than the pit aperture among the 40 conifer species sampled here (51% larger on average), which may prevent the torus from passing through the aperture. However, this size difference

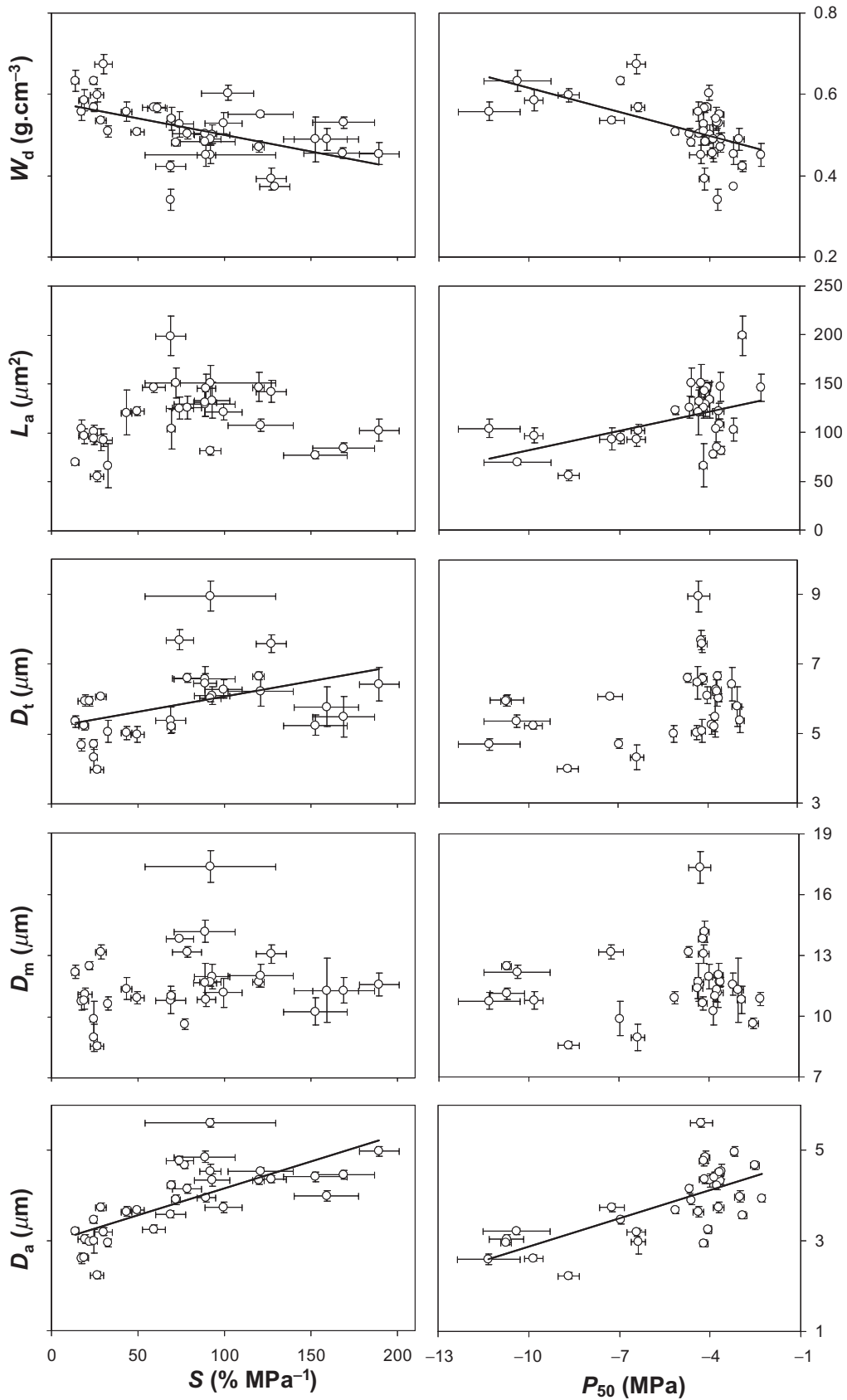


Figure 5. Relationships between wood density (W_d , a), lumen area (L_a , b), torus diameter (D_t , c), pit membrane diameter (D_m , d), pit aperture diameter (D_a , e) and parameters of cavitation resistance (P_{50} and S). Error bars represent SE. Regression line is indicated when the correlation is significant ($P < 0.05$).

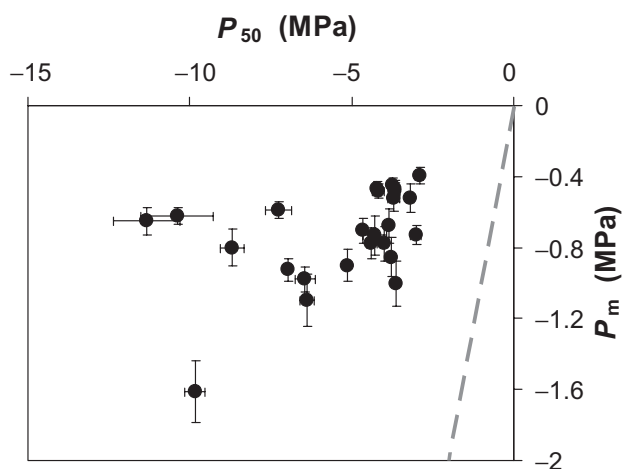


Figure 6. Capillary-seeding pressure of the margo (P_m) versus xylem pressure inducing 50% loss in conductance (P_{50}). Grey dashed line represent 1:1 relationship.

does not ensure that the torus might not move off-center. Further investigations are needed to investigate this possibility, particularly by estimating more accurately the margo elasticity (see Hacke *et al.* 2004) and the margo deflected distance in the pit chamber. Indeed, margo elasticity depends on the modulus of elasticity of the microfibril spokes, the strain of the strands, the cross-sectional area of the strands and the total number of strands supporting the torus.

Seal capillary-seeding

Our data showed that cavitation resistance increased with increasing torus overlap (i.e. increased torus diameter

relative to the pit aperture). This result is in agreement with previous findings. Indeed, Hacke & Jansen (2009) reported a weak correlation between the torus overlap and cavitation resistance for three conifer species, resulting in a similar trend to the one we report here (roots tended to have smaller overlap and cavitation resistance than stems). Domec *et al.* (2008) showed that in tall Douglas-fir trees (*Pseudotsuga menziesii*) there was a significant increase in the torus overlap with increasing tree height concurrent with an increase in cavitation resistance. A recent study from Schoonmaker *et al.* (2010) also reported that the torus overlap was significantly larger in open-grown, cavitation resistant individuals compared with understory, less resistant ones. Overall, these results support the hypothesis of seal capillary-seeding, and suggest that the adhesion of the torus to the pit border (i.e. airtightness of the torus – inner wall interface) might be the main determinant of cavitation resistance. Even though the surface tension is presumably sufficiently large to bring the torus into contact with the pit border, adhesive forces between the torus and pit border might be too weak (Comstock & Côté Jr 1968). This could be due to a low margo elasticity preventing the torus from being tightly aspirated. As a tight aspiration is inferred when the imprint of the pit aperture on the torus is clearly visible (Comstock & Côté Jr 1968), detailed studies in different species using scanning electron microscopy are needed to test whether the torus is tightly sealed against the pit border.

Other studies using scanning microscopy have shown that the torus and the inner wall of the pit membrane never appear perfectly smooth such that air seeding could occur through these tiny pores (Kitin *et al.* 2009). Indeed, the presence of warts on the inner wall of the pit membrane can prevent a perfect seal, and thus permit seepage through the

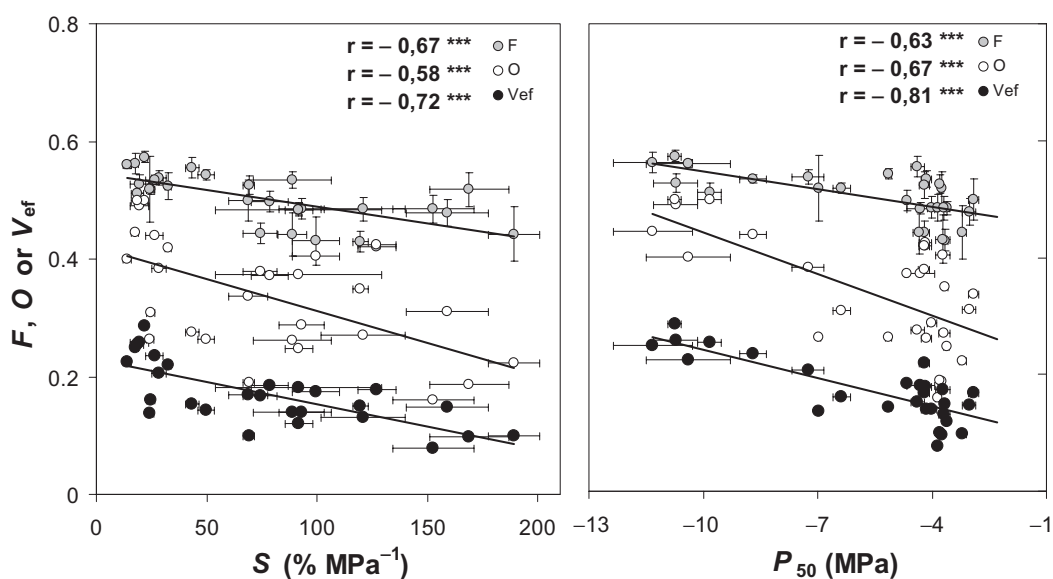


Figure 7. Relationships between functional properties of the bordered pit (torus overlap, O , open circles; margo flexibility, F , grey circles; valve effect, V_{ef} , black circles) and cavitation-resistance parameters (P_{50} and S). Error bars represent SE. Pearson correlation coefficients (r) are indicated, * $P < 0.05$; ** $P < 0.01$; *** $P < 0.001$.

pit (Côté Jr 1963). Following the Young-Laplace law, the measured P_{50} values correspond to capillary failures of 20 and 100 nm menisci for *C. glabra* and *M. glyptstroides*, respectively. The presence of these tiny pores has never been investigated and requires therefore more attention. Most recently, the presence of pores extending throughout the entire torus wall has also been observed in *pinus pinaster* trees. These pores were found on a large number of tori and on different individuals, ranging between 20 to 150 nm of diameter (Delzon, personal observations). Such pores were also reported on two conifer species: *Abies sachalinensis* (Sano, Kawakami & Ohtani 1999) and *P. wallichiana* (Jansen *et al.* 2008). Given the size of these pores, air seeding could theoretically occur through the torus by capillary failure. However, current investigations on Cupressaceae species do not seem to confirm this hypothesis and torus thickness was found to be negatively correlated with cavitation resistance (Hacke & Jansen 2009); the thinner the torus, the more cavitation resistant the species.

The valve effect theory

In light of the results reported here and elsewhere, the valve effect is emerging as the pit functional trait best correlated with cavitation resistance and might explain the air-seeding resistance of bordered pit membranes. This result suggests that pit air-seeding resistance is determined by: (1) a flexible margo allowing the torus to move against the pit border; and (2) a wide torus relatively to the pit aperture to ensure an airtight seal around the pit aperture. A different overlap index was proposed by Hacke *et al.* (2004), corresponding to the variation of the torus diameter relative to the pit membrane and pit aperture diameters. This relative overlap $[D_t - D_a]/[D_m - D_a]$ is exactly the fraction of the pit border width that is covered by the torus. However, using this relative index, we found a weaker correlation with both P_{50} and slope compared with the torus overlap we have used (data not shown). This finding is consistent with the latter work of Hacke & Jansen (2009), who found no correlation between the relative overlap and P_{50} , whereas this index seemed to be more correlated with pit hydraulic conductivity.

The comparison of cavitation resistance traits with xylem anatomy and pit functional properties carried out on a broad range of conifer species from six families confirms the key role of the torus-pit membrane apparatus in cavitation resistance. Although our results show that the valve effect, determined by: (1) the deflection capacity of the membrane; and (2) the seal capacity of the torus-pit aperture, is the best predictor of cavitation resistance, additional work is necessary to confirm this theory. In particular, work focusing on the microfibril physical properties and their elastic modulus is required. Here, by a process of elimination, we identified the seal capillary-seeding as the most likely mode of air-seeding in bordered pit of conifer species. However, we cannot reject the hypothesis of torus capillary-seeding and more information on the structural properties of tori is required based on direct observations using

transmission electron microscopy. In addition, the mechanical properties of the tracheids (wood density and structure) could play a key role in preventing conduit collapse. For instance, greater tracheid wall thickness would be necessary to resist implosion by negative pressure (Hacke *et al.* 2001). Significant relationships between wood density, lumen area and cavitation resistance were found in the present study and therefore further investigations would be of great interest to estimate the wall implosion pressure and the thickness-to-span ratio.

ACKNOWLEDGMENTS

This study was supported by a Fulbright-Aquitaine fellowship and an INRA innovative project.

REFERENCES

- Bailey I.W. (1916) The structure of the bordered pits of conifers and its bearing upon the tension hypothesis of the ascent of sap in plants. *Botanical Gazette* **62**, 133–142.
- Bauch J., Liese W. & Schultze R. (1972) The morphological variability of the bordered pit membranes in gymnosperms. *Wood Science and Technology* **6**, 165–184.
- Brodribb T.J. & Cochard H. (2009) Hydraulic failure defines the recovery and point of death in water-stressed conifers. *Plant Physiology* **149**, 575–584.
- Christman M.A., Sperry J.S. & Adler F.R. (2009) Testing the 'rare pit' hypothesis for xylem cavitation resistance in three species of *Acer*. *New Phytologist* **182**, 664–674.
- Cochard H. (2002) A technique for measuring xylem hydraulic conductance under high negative pressures. *Plant, Cell & Environment* **25**, 815–819.
- Cochard H. (2006) Cavitation in trees. *Comptes Rendus Physique* **7**, 1018–1026.
- Cochard H., Cruizat P. & Tyree M.T. (1992) Use of positive pressures to establish vulnerability curves. Further support for the air-seeding hypothesis and implications for pressure-volume analysis. *Plant Physiology* **100**, 205–209.
- Cochard H., Damour G., Bodet C., Tharwat I., Poirier M. & Ameglio T. (2005) Evaluation of a new centrifuge technique for rapid generation of xylem vulnerability curves. *Physiologia Plantarum* **124**, 410–418.
- Cochard H., Holtta T., Herbette S., Delzon S. & Mencuccini M. (2009) New insights into the mechanisms of water-stress-induced cavitation in conifers. *Plant Physiology* **151**, 949–954.
- Comstock G.L. & Côté W.A. Jr (1968) Factors affecting permeability and pit aspiration in coniferous sapwood. *Wood Science and Technology* **2**, 279–291.
- Côté W.A. Jr (1963) Structural factors affecting the permeability of wood. *Journal of Polymer Science Part C: Polymer Symposia* **2**, 231–242.
- Crombie D.S., Hipkins M.F. & Milburn J.A. (1985) Gas penetration of pit membranes in the xylem of *Rhododendron* as the cause of acoustically detectable sap cavitation. *Australian Journal of Plant Physiology* **12**, 445–453.
- Domec J.C. & Gartner B.L. (2002) Age- and position-related changes in hydraulic versus mechanical dysfunction of xylem: inferring the design criteria for Douglas-fir wood structure. *Tree Physiology* **22**, 91–104.
- Domec J.C., Lachenbruch B. & Meinzer F.C. (2006) Bordered pit structure and function determine spatial patterns of air-seeding thresholds in xylem of Douglas-fir (*Pseudotsuga menziesii*; Pinaceae) trees. *American Journal of Botany* **93**, 1588–1600.

- Domec J.C., Lachenbruch B., Meinzer F.C., Woodruff D.R., Warren J.M. & McCulloh K.A. (2008) Maximum height in a conifer is associated with conflicting requirements for xylem design. *Proceedings of the National Academy of Sciences of the United States of America* **105**, 12069–12074.
- Farjon A. (2008) *A Natural History of Conifers*. Timber Press, Inc., Portland, OR, USA.
- Gregory S.C. & Petty J.A. (1973) Valve action of bordered pits in conifers. *Journal of Experimental Botany* **24**, 763–765.
- Hacke U.G. & Jansen S. (2009) Embolism resistance of three boreal conifer species varies with pit structure. *New Phytologist* **182**, 675–686.
- Hacke U.G., Sperry J.S., Pockman W.T., Davis S.D. & McCulloh K.A. (2001) Trends in wood density and structure are linked to prevention of xylem implosion by negative pressure. *Oecologia* **126**, 457–461.
- Hacke U.G., Sperry J.S. & Pittermann J. (2004) Analysis of circular bordered pit function – II. Gymnosperm tracheids with torus-margo pit membranes. *American Journal of Botany* **91**, 386–400.
- Jansen S., Pletsers A. & Sano Y. (2008) The effect of preparation techniques on SEM-imaging of pit membranes. *Iawa Journal* **29**, 161–178.
- Jarbeau J.A., Ewers F.W. & Davis S.D. (1995) The mechanism of water-stress-induced embolism in 2 species of chaparral shrubs. *Plant, Cell & Environment* **18**, 189–196.
- Kitin P., Fujii T., Abe H. & Takata K. (2009) Anatomical features that facilitate radial flow across growth rings and from xylem to cambium in *Cryptomeria japonica*. *Annals of Botany* **103**, 1145–1157.
- Maherali H., Pockman W.T. & Jackson R.B. (2004) Adaptive variation in the vulnerability of woody plants to xylem cavitation. *Ecology* **85**, 2184–2199.
- Martinez-Vilalta J., Sala A. & Pinol J. (2004) The hydraulic architecture of Pinaceae – a review. *Plant Ecology* **171**, 3–13.
- Pammenter N.W. & Vander Willigen C. (1998) A mathematical and statistical analysis of the curves illustrating vulnerability of xylem to cavitation. *Tree Physiology* **18**, 589–593.
- Petty J.A. (1972) The aspiration of bordered pits in conifer wood. *Proceedings of the Royal Society B-Biological Sciences* **181**, 395–406.
- Pinol J. & Sala A. (2000) Ecological implications of xylem cavitation for several Pinaceae in the Pacific Northern USA. *Functional Ecology* **14**, 538–545.
- Pittermann J., Sperry J.S., Hacke U.G., Wheeler J.K. & Sikkema E.H. (2005) Torus-margo pits help conifers compete with angiosperms. *Science* **310**, 1924–1924.
- Pittermann J., Sperry J.S., Hacke U.G., Wheeler J.K. & Sikkema E.H. (2006a) Inter-tracheid pitting and the hydraulic efficiency of conifer wood: the role of tracheid allometry and cavitation protection. *American Journal of Botany* **93**, 1265–1273.
- Pittermann J., Sperry J.S., Wheeler J.K., Hacke U.G. & Sikkema E.H. (2006b) Mechanical reinforcement of tracheids compromises the hydraulic efficiency of conifer xylem. *Plant, Cell & Environment* **29**, 1618–1628.
- Sachs I.B. (1963) Torus of the bordered-pit membrane in conifers. *Nature* **198**, 906–907.
- Sano Y., Kawakami Y. & Ohtani J. (1999) Variation in the structure of intertracheary pit membranes in *Abies sachalinensis*, as observed by field-emission scanning electron microscopy. *Iawa Journal* **20**, 375–388.
- Schoonmaker A.L., Hacke U.G., Landhausser S.M., Lieffers V.J. & Tyree M.T. (2010) Hydraulic acclimation to shading in boreal conifers of varying shade tolerance. *Plant, Cell & Environment* **33**, 382–393.
- Sperry J.S. & Tyree M.T. (1990) Water-stress-induced xylem embolism in three species of conifers. *Plant, Cell & Environment* **13**, 427–436.
- Tyree M.T. & Zimmermann M.H. (2002) *Xylem Structure and the Ascent of Sap*. Springer, Berlin, Germany.
- Wheeler J.K., Sperry J.S., Hacke U.G. & Hoang N. (2005) Inter-vessel pitting and cavitation in woody Rosaceae and other vesselless plants: a basis for a safety versus efficiency trade-off in xylem transport. *Plant, Cell & Environment* **28**, 800–812.

Received 6 April 2010; received in revised form 2 July 2010; accepted for publication 5 July 2010

SUPPORTING INFORMATION

Additional Supporting Information may be found in the online version of this article:

Appendix S1. Study species.

Appendix S2. Mean values of parameters of cavitation resistance (P_{50} and S), wood density (W_d), lumen area (L_a), pit aperture diameter (D_a), torus diameter (D_t) and pit membrane diameter (D_m) for each species. Values in brackets represent standard errors of the mean.

Please note: Wiley-Blackwell are not responsible for the content or functionality of any supporting materials supplied by the authors. Any queries (other than missing material) should be directed to the corresponding author for the article.